

A randomized clinical trial of lipid metabolism modulation with fenofibrate for acute coronavirus disease 2019

Received: 5 August 2022

A list of authors and their affiliations appears at the end of the paper

Accepted: 21 October 2022

Published online: 7 November 2022

 Check for updates

Severe acute respiratory syndrome coronavirus 2 (SARS-CoV-2) cytotoxicity may involve inhibition of peroxisome proliferator-activated receptor alpha. Fenofibrate activates peroxisome proliferator-activated receptor alpha and inhibits SARS-CoV-2 replication in vitro. Whether fenofibrate can be used to treat coronavirus disease 2019 (COVID-19) infection in humans remains unknown. Here, we randomly assigned inpatients and outpatients with COVID-19 within 14 d of symptom onset to 145 mg of oral fenofibrate nanocrystal formulation versus placebo for 10 d, in a double-blinded fashion. The primary endpoint was a severity score whereby participants were ranked across hierarchical tiers incorporating time to death, mechanical ventilation duration, oxygenation, hospitalization and symptom severity and duration. In total, 701 participants were randomized to fenofibrate ($n = 351$) or placebo ($n = 350$). The mean age of participants was 49 ± 16 years, 330 (47%) were female, mean body mass index was $28 \pm 6 \text{ kg/m}^2$ and 102 (15%) had diabetes. Death occurred in 41 participants. Compared with placebo, fenofibrate had no effect on the primary endpoint. The median (interquartile range) rank in the placebo arm was 347 (172, 453) versus 345 (175, 453) in the fenofibrate arm ($P = 0.819$). There was no difference in secondary and exploratory endpoints, including all-cause death, across arms. There were 61 (17%) adverse events in the placebo arm compared with 46 (13%) in the fenofibrate arm, with slightly higher incidence of gastrointestinal side effects in the fenofibrate group. Overall, among patients with COVID-19, fenofibrate has no significant effect on various clinically relevant outcomes ([NCT04517396](#)).

Infection with SARS-CoV-2, the virus responsible for COVID-19, is an important public health problem. Available data suggest that COVID-19 progression is dependent on metabolic mechanisms¹. Individuals with COVID-19 who developed acute respiratory distress syndrome and death are characterized by older age and a higher prevalence of hypertension, obesity, diabetes and cardiovascular diseases compared to individuals with milder disease^{1–6}. Hyperglycaemia and hyperlipidaemia are also risk factors for acute respiratory distress in

patients with COVID-19 disease^{1,7}. Indeed, type 2 diabetes mellitus and the metabolic syndrome are associated with a markedly increased risk of death in the setting of COVID-19 (refs. ^{1,8}).

Several experimental studies suggest a mechanistic link between abnormal metabolism and the severity of SARS-CoV-2 and other coronavirus infections. Palmitoylation of the SARS-CoV-2 spike protein has been shown to be essential for virus–cell fusion and infectivity^{8–10}. Gene expression analyses in cultured human bronchial cells infected with

Table 1 | General characteristics of study participants

Variable	Total (n=701)	Placebo (n=350)	Fenofibrate (n=351)
Age, years	49 (16)	49 (16)	49 (16)
Female sex	330 (47%)	164 (47%)	166 (47%)
Race/ethnicity			
Non-Hispanic black	47 (7%)	23 (7%)	24 (7%)
Non-Hispanic white	263 (38%)	135 (39%)	128 (37%)
Hispanic	350 (50%)	173 (49%)	177 (51%)
Other	40 (6%)	19 (5%)	21 (6%)
Hypertension	186 (27%)	98 (28%)	88 (25%)
Diabetes mellitus	102 (15%)	58 (17%)	44 (13%)
On insulin	20 (20%)	12 (21%)	8 (18%)
High cholesterol	96 (14%)	56 (16%)	40 (11%)
Ischaemic heart disease	47 (7%)	31 (9%)	16 (5%)
Heart failure	19 (3%)	9 (3%)	10 (3%)
Atrial fibrillation	14 (2%)	8 (2%)	6 (2%)
Previous pulmonary embolism or deep vein thrombosis	14 (2%)	9 (3%)	5 (1%)
Obstructive sleep apnea	23 (3%)	15 (4%)	8 (2%)
Chronic pulmonary disease	82 (12%)	43 (12%)	39 (11%)
Current smoker	67 (10%)	34 (10%)	33 (9%)
Illicit drug use	11 (2%)	5 (1%)	6 (2%)
Fully vaccinated against SARS-CoV-2	319 (46%)	156 (45%)	163 (46%)
SARS-CoV-2 diagnosed using real-time PCR testing	438 (62%)	210 (60%)	228 (65%)
Dyspnoea severity, 0–10 Borg scale	2.2 (2.6)	2.3 (2.7)	2.0 (2.5)
Cough severity, 0–10 scale	3.8 (2.9)	3.8 (3.0)	3.8 (2.8)
Chest pain severity, 0–10 scale	1.6 (2.5)	1.7 (2.6)	1.5 (2.4)
Myalgias severity, 0–10 scale	2.9 (3.0)	3.0 (3.1)	2.8 (2.9)
Fatigue severity, 0–10 scale	3.6 (3.1)	3.6 (3.0)	3.6 (3.2)
Multifocal infiltrates on chest imaging	185 (62%)	88 (62%)	97 (61%)
Oxygen saturation, %	96 (3)	96 (3)	96 (3)
Oxygen supplementation	230 (33%)	118 (34%)	112 (32%)
Systolic blood pressure, mm Hg	123 (16)	123 (16)	123 (16)
Diastolic blood pressure, mm Hg	76 (31)	76 (31)	76 (30)
Heart rate, beats per minute	82 (13)	82 (14)	82 (12)
BMI, kg/m ²	28 (6)	28 (6)	28 (6)
eGFR, ml min ⁻¹ per 1.73 m ²	101 (20)	101 (21)	100 (20)
Leucocyte count, 10 ⁹ cells/l	1,287 (3,053)	1,346 (3,147)	1,231 (2,965)
Platelets, 10 ³ cells/μl	227 (86)	226 (91)	228 (81)
C-reactive protein, mg dl ⁻¹	43 (73)	42 (68)	45 (78)
Days from admission to randomization	2 (3)	2 (3)	2 (2)
Days from symptom onset to randomization	7 (4)	7 (4)	7 (4)
Inpatient	302 (43%)	151 (43%)	151 (43%)
Total days on drug	9 (3)	9 (3)	9 (3)
Dropouts	17 (2%)	9 (3%)	8 (2%)

Results are presented as number (proportion) for binary or categorical variables and mean (standard deviation) for continuous variables. Proportions were calculated using the number of individuals with the characteristic divided by the number of participants with non-missing data about the characteristic. eGFR, estimated glomerular filtration rate.

SARS-CoV-2 as well as lung tissue from patients with COVID-19 indicated a marked shift in cellular metabolism, with excessive intracellular lipid generation¹¹. In further cell culture experiments, the peroxisome proliferator-activated receptor alpha (PPAR-α) agonist fenofibrate (a widely available low-cost generic drug approved by the US Food and Drug Administration and multiple other regulatory agencies around the

world to treat dyslipidaemias) reversed the metabolic changes induced by SARS-CoV-2, and inhibited viral production/replication¹¹. In more recent cell culture experiments, fenofibric acid, the active form of fenofibrate, induced destabilization of the SARS-CoV-2 viral spike (S) protein and reduction of viral infection¹². Fibrates also appear to exert immunomodulatory effects that could be beneficial in COVID-19 disease^{13–15}.

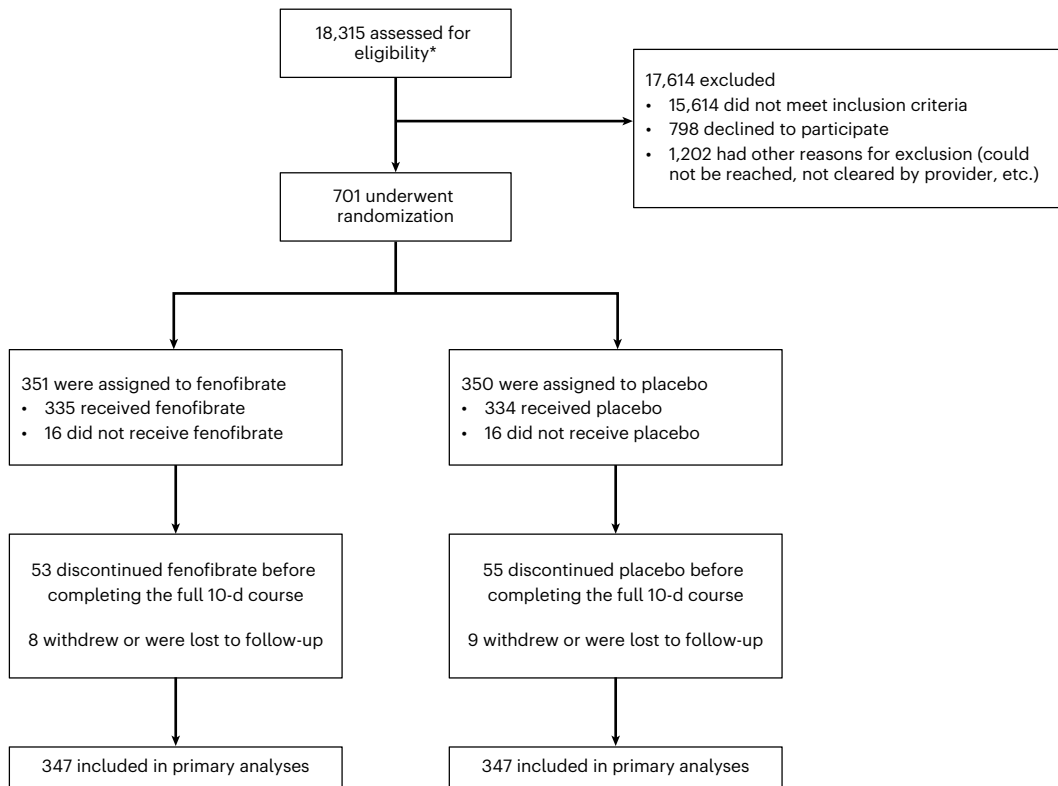


Fig. 1 | Participant enrolment, randomization and follow-up in the FEnofibRate as a Metabolic INtervention for COVID-19 (FERMIN) trial.

These preclinical studies suggesting that fenofibrate could directly target host metabolic pathways as well as viral proteins to minimize SARS-CoV-2 replication and possibly suppress its pathogenesis in respiratory tract tissue, motivated a rigorously designed, international multicentre clinical trial to assess the potential efficacy of fenofibrate in COVID-19 in humans. The aim of this randomized controlled trial was to assess whether fenofibrate improves clinical outcomes in patients with COVID-19.

Results

Study participants

A total of 701 participants were enrolled and randomized (156 in Colombia, 133 in Greece, 116 in the United States, 116 in Peru, 113 in Lebanon and 67 in Mexico). Participants were enrolled from October 2, 2020 to February 27, 2022. General characteristics of study participants are shown in Table 1. The mean age of enrolled participants was 49 ± 16 years, 330 (47%) were female, mean body mass index (BMI) was 28 ± 6 kg/m 2 , 102 (15%) had a history of diabetes mellitus, 47 (7%) had a history of ischaemic heart disease, 186 (27%) had a history of hypertension and 302 (43%) were enrolled as inpatients. Initial mean oxygen saturation was $97\% \pm 3\%$ among participants enrolled as outpatients and $95\% \pm 3\%$ among those enrolled as inpatients; 71% of inpatients were on oxygen supplementation at the time of enrolment. A total of 351 participants were randomized to fenofibrate and 350 participants were randomized to placebo (Fig. 1). Only 17 participants (2%) were excluded, withdrew following randomization or were lost to follow-up. The majority of participants ($n = 438$; 62%) were positive for SARS-CoV-2 by real-time PCR testing, while the remainder were positive by rapid antigen testing.

Primary endpoint

In the primary intent-to-treat analyses, the distribution of the ranked severity scores between participants assigned to fenofibrate versus

placebo was remarkably similar. The median (interquartile range (IQR)) ranked severity score in the placebo arm was 347 (172, 453) versus 345 (175, 453) in the fenofibrate arm ($P = 0.819$), where a lower value signifies more severe COVID-19 course (Table 2 and Fig. 2a). After adjusting for age, sex, inpatient versus outpatient status, baseline inspired concentration of oxygen/percentage oxygen saturation (FiO $_2$ /SpO $_2$) ratio, race, ethnicity, BMI, baseline diabetes status and country, and clustered by site, participants assigned to fenofibrate exhibited mean ranked severity scores that were 0.03 (95% CI –0.05, 0.11) units higher than those assigned to control ($P = 0.448$). The individual components of the ranked severity score are described in Extended Data Table 1.

Secondary and exploratory endpoints

The number of days alive, out of the intensive care unit (ICU), free of mechanical ventilation (invasive and noninvasive), extracorporeal membrane oxygenation (ECMO) or maximal available respiratory support in the 30 d following randomization was similar among the arms (median time in both arms, 30 (IQR 30, 30); $P = 0.134$). The seven-category WHO (World Health Organization) ordinal scale was similar between the arms (placebo median 1 (IQR 1, 2); fenofibrate median 1 (IQR 1, 1); P value 0.246). Similarly, the modified ranked severity scores (constructed like the primary endpoint but using a more comprehensive COVID-19 symptom scale instead of the dyspnoea Borg scale) were very similar across arms (placebo median score 358 (IQR 174, 513); fenofibrate median score 343 (IQR 177, 525); P value 0.740).

Kaplan–Meier curves for deaths in the two arms are shown in Fig. 2b. A total of 41 deaths occurred; 22 in the placebo arm and 19 in the fenofibrate arm (hazard ratio (HR) 0.880 (95% confidence interval (CI) = 0.465, 1.663); $P = 0.693$). After adjusting for age, sex, inpatient versus outpatient status, baseline FiO $_2$ /SpO $_2$, race, ethnicity, BMI, baseline diabetes status and country, and clustered by site, there was no significant difference in all-cause death at 30 d between the arms

Table 2 | Comparison of secondary and exploratory endpoints between fenofibrate versus placebo*

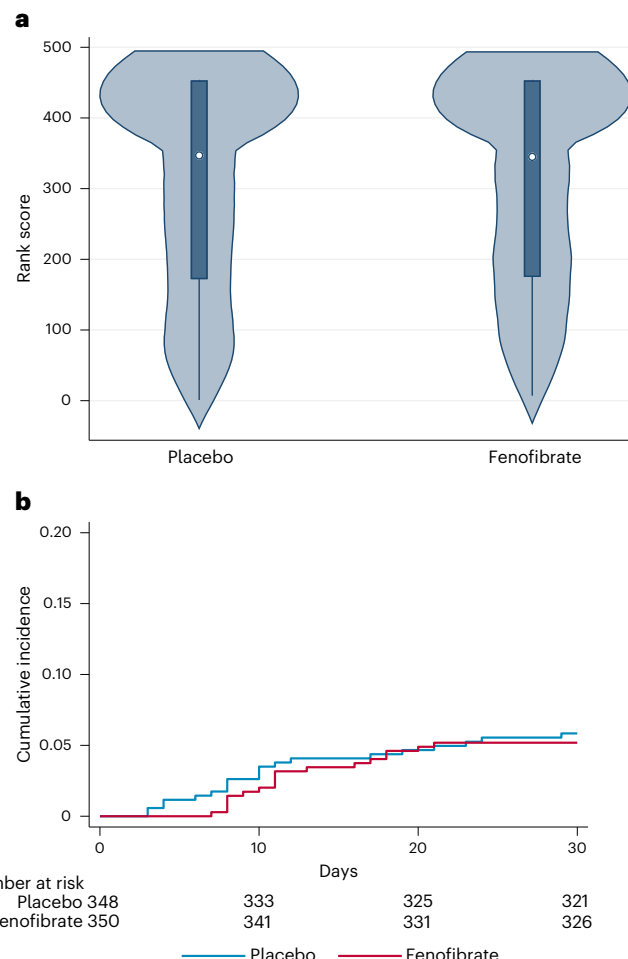
Endpoint	Wilcoxon rank-sum test			Adjusted linear regression	
	Fenofibrate median (IQR)	Placebo median (IQR)	P value	Effect size β of fenofibrate versus placebo (95% CI)	P value
Primary endpoint					
Global ranked severity score	5.32 (2.98, 6.00)	5.33 (2.98, 6.00)	0.819	0.03 (-0.05, 0.11)	0.448
Secondary endpoints					
Number of days alive, out of ICU/ECMO/invasive ventilation	30 (30, 30)	30 (30, 30)	0.134	0.54 (-0.21, 1.29)	0.157
WHO ordinal scale	1 (1, 1)	1 (1, 2)	0.246	-0.08 (-0.25, 0.09)	0.367
Modified ranked severity score (COVID-19 symptom scale instead of Borg)	5.05 (2.98, 5.22)	5.05 (2.98, 5.21)	0.928	0.03 (-0.05, 0.11)	0.440
Exploratory endpoints					
Number of days alive and out of the hospital at 30 d	30 (25, 30)	30 (25, 30)	0.834	0.22 (-0.44, 0.88)	0.5
Modified ranked severity score with only factors 1–4	5.03 (2.98, 5.03)	5.03 (2.98, 5.03)	0.776	0.03 (-0.04, 0.10)	0.387

All results represent two-sided statistical testing. All linear regression models were prespecified. The beta coefficients represent the effect of intervention group (fenofibrate versus placebo) on the indicated endpoint, adjusted by the prespecified covariates (age, sex, inpatient versus outpatient status, baseline $\text{FiO}_2/\text{SpO}_2$, race, ethnicity, BMI, baseline diabetes status and country) and clustered by site. Severity scores were condensed by level of the hierarchical outcome for clarity of interpretation in the regression models (that is, those who died have a score beginning with 0; those who did not die but were mechanically ventilated have a score beginning with 1). For analyses related to all-cause death, hospitalization and discharge, see the Results.

(adjusted HR 0.983; 95% CI 0.562, 1.718; $P = 0.952$). The Kaplan–Meier failure estimates were not significantly different between the arms ($P = 0.692$).

The number of days alive and out of the hospital during the 30 d following randomization were similar between the two arms (median days in the placebo arm, 30 (IQR 25, 30); median days in the fenofibrate arm, 30 (IQR 25, 30); $P = 0.834$). The additional modified ranked severity score (similar to the primary endpoint, but built only with factors 1–4) was similar across the arms (placebo median score 317 (IQR 172, 317); fenofibrate median score 317 (IQR 175, 317); $P = 0.836$). In analyses restricted to the 398 participants enrolled as outpatients, the risk of hospitalization was not significantly different in participants randomized to fenofibrate compared with placebo (1 versus 4 participants hospitalized; unadjusted HR 0.249; 95% CI 0.028, 2.227; $P = 0.214$; Extended Data Fig. 1). In analyses restricted to the 302 participants enrolled as inpatients, the cause-specific hazard for hospital discharge, considering death as a competing risk, was essentially identical between the arms (unadjusted HR 1.001; 95% CI 0.792, 1.267; $P = 0.990$; Extended Data Fig. 2).

Analyses of all secondary and exploratory endpoints via prespecified linear regression analyses that adjusted for age, sex, inpatient versus outpatient status, baseline $\text{FiO}_2/\text{SpO}_2$, race, ethnicity, BMI, baseline diabetes status and country, and clustered by site, were consistent with the primary results obtained with the van Elteren test (Table 2).

**Fig. 2 | Key outcomes among participants in each randomization arm.**

a, Distribution of the primary endpoint (ranked severity score) between the randomization arms (placebo $N = 347$ participants; fenofibrate $N = 347$ participants). The y axis represents the range of ranked severity scores, and the x axis represents the frequency density of distributions of the ranks in each treatment arm. The white dot represents the median ranked severity score, the solid box represents the IQR, and the vertical lines represent the upper-adjacent and lower-adjacent values. The upper-adjacent value and the IQR values were identical. **b**, Cumulative incidence for all-cause death at 30 d.

Prespecified subgroup analyses

There was no evidence of effect modification (Fig. 3) by age, sex, race, diabetes status, obesity status, inpatient versus outpatient status at the time of enrolment, $\text{FiO}_2/\text{SpO}_2$ at the time of enrolment (< versus \geq median), duration of symptoms (<7 versus ≥ 7 d), WHO disease severity, country, formulation, adherence to therapy or compound (fenofibrate versus fenofibric acid).

Adverse events

There were 61 (17%) adverse events in the placebo arm compared with 46 (13%) in the fenofibrate arm (Extended Data Table 2). There were no appreciable differences in the incidence of adverse events classified by organ system, except for a slightly greater incidence of gastrointestinal adverse events with fenofibrate (9 events (3%) in the placebo arm; 19 (5%) in the fenofibrate arm).

Discussion

We performed an international multicentre randomized placebo-controlled clinical trial designed to evaluate the clinical efficacy of fenofibrate on COVID-19 severity. Our trial, which enrolled both

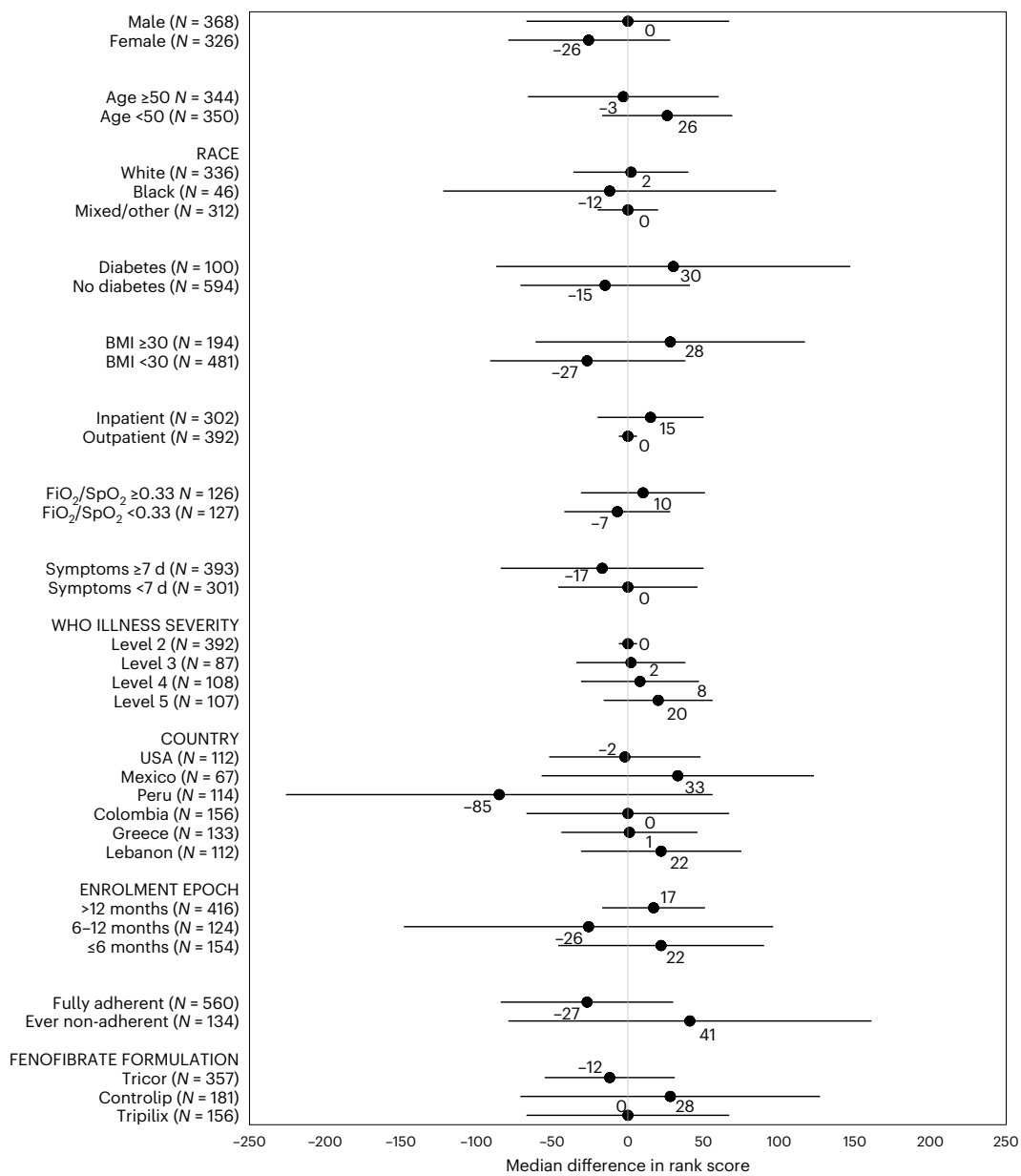


Fig. 3 | Forest plot of the differences in ranked severity scores across subgroups. The plot represents the differences in median ranked severity scores between participants randomized to fenofibrate versus placebo in each subgroup. Positive values indicate better outcomes in the fenofibrate arm.

Negative values indicate better outcomes in the placebo group. The central dot represents the difference in median scores and the error bars represent the 95% CIs.

inpatients and outpatients, did not demonstrate any appreciable effect of fenofibrate on the trial primary endpoint, which evaluated multiple facets of COVID-19 severity, including death, invasive and noninvasive mechanical ventilatory support, duration of hospitalization among inpatients, time to hospitalization among outpatients and symptom severity among outpatients who were not hospitalized. Multiple pre-specified sensitivity, secondary and subgroup analyses corroborated the primary analyses. Over 30 d of follow-up after randomization, we observed no significant effect of fenofibrate therapy on the number of days alive, out of the ICU and free of invasive mechanical ventilation, on the WHO ordinal outcome scale, nor on number of days alive and out of the hospital. Similarly, there was no significant difference observed when the ranked severity score incorporated a multifactorial COVID-19 symptom score instead of the Borg score or if the ranked severity score was restricted to only objective outcome measures (that is, when the symptom score was omitted).

Our study was motivated by various epidemiological and *in vitro* observations suggesting a link between abnormal lipid metabolism and the pathogenesis of SARS-CoV-2 infection or severity of COVID-19, as well as *in vitro* studies in which an antiviral effect of fenofibrate has been reported. Abnormal lipid metabolism has been shown to be involved in the cellular pathogenesis of SARS-CoV-2 and other RNA viruses. Nardacci et al. demonstrated that SARS-CoV-2 infection induces a striking accumulation of lipid droplets in cultured Vero E6 cells, as well as type II pneumocytes from infected patients¹⁶. Although this phenomenon was reported to constitute a major difference compared to SARS-CoV-1 infection, it does not appear to be unique to SARS-CoV-2, because marked alterations in lipid metabolism have been shown to occur as a consequence of hepatitis C virus infection¹⁷, as well as human coronavirus 229E¹⁸ and some picornaviruses¹⁹.

Given the potential role of dysregulated lipid metabolism in SARS-CoV-2 infection, there is substantial interest in the potential

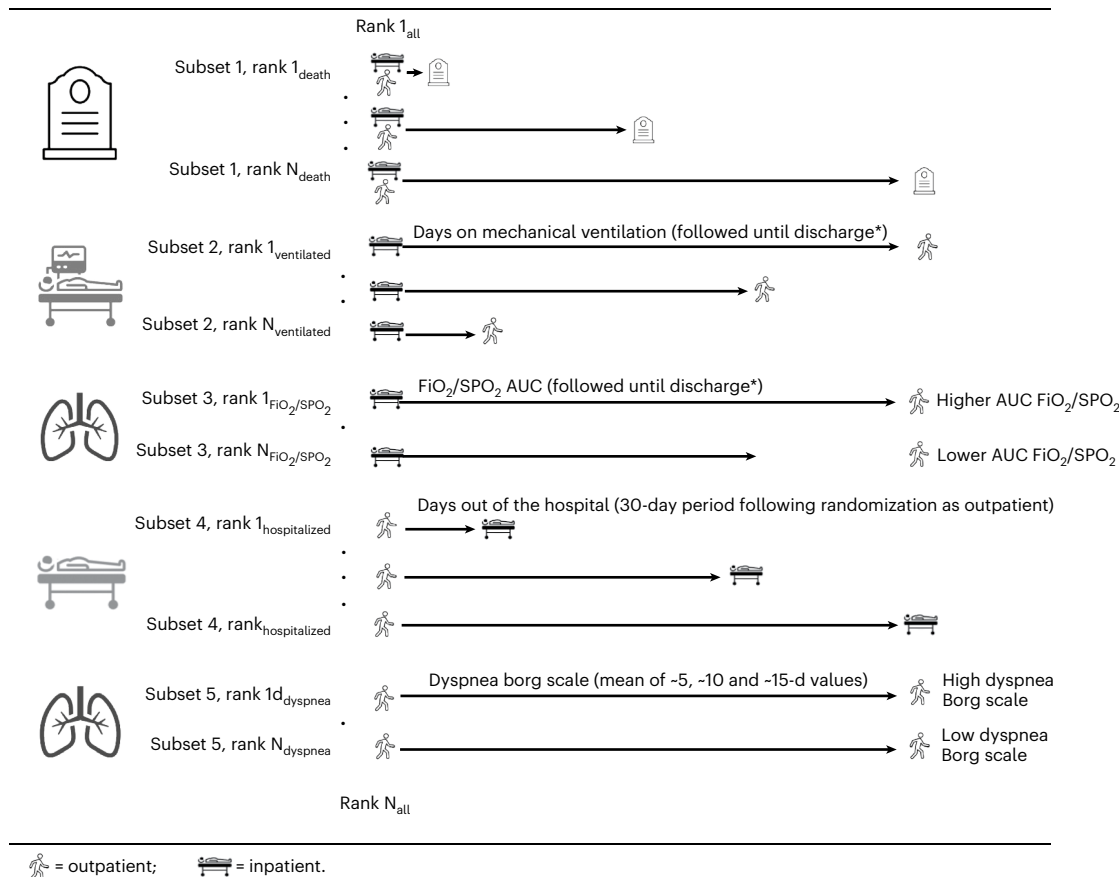


Fig. 4 | Primary endpoint of the trial (ranked severity score). Participants were ranked hierarchically according to their clinical course. The primary endpoint of the trial was a global rank score that ranked patient outcomes according to five factors, shown as tiers from top to bottom (labelled as subsets 1–5). The left-sided icons (walking person and person in hospital bed) indicate the participant status at the time of enrolment (outpatient and inpatient, respectively). The top tier included inpatients and outpatients, whereas other subsets included inpatients or outpatients, but not both. Outcomes of hypothetical participants are represented within each tier by the right-pointing arrows. The icons on the right of the arrows represent the participant status at trial completion or at the time of the relevant outcome event (such as death, hospital discharge or hospital admission). Participants were ranked within each tier according to the following specific criteria: tier 1, time to death (ranked from shortest to longest, up to 30 d

after randomization); tier 2, for participants enrolled as inpatients, the number of days supported by mechanical ventilation (invasive or noninvasive) or ECMO (until hospital discharge, up to 30 d after randomization, ranked from longest to shortest); tier 3, for participants enrolled as inpatients who did not require mechanical ventilation or ECMO, the $\text{FiO}_2/\text{SpO}_2$ ratio area under the curve until hospital discharge, up to 30 d after randomization, ranked from highest to lowest; tier 4, for participants enrolled as outpatients who were subsequently hospitalized, the number of days out of the hospital during the 30-d period following randomization (ranked from lowest to highest); tier 5, for participants enrolled as outpatients who did not get hospitalized during the 30 d observation period, the modified dyspnoea Borg scale (mean value of assessments at -5, -10 and -15 d, ranked from highest to lowest). AUC, area under the curve.

antiviral role of medications that affect lipid metabolism. Davies et al. recently reported an effect of fenofibric acid (the active metabolite of fenofibrate) on the dimerization of angiotensin-converting enzyme 2, the cellular receptor for SARS-CoV-2 (ref. ¹²). Fenofibric acid was also reported to destabilize the receptor-binding domain of the SARS-CoV-2 spike protein and to inhibit binding of the S protein receptor-binding domain to angiotensin-converting enzyme 2. The investigators subsequently assessed the effect of fenofibrate and fenofibric acid in cultured Vero cells infected with SARS-CoV-2. They reported that both fenofibrate and fenofibric acid were able to reduce viral infection rates. However, the relative effect of fenofibrate versus fenofibric acid appeared to vary across experimental assays, which also utilized one of two different SARS-CoV isolates. A preliminary non-peer-reviewed publication by Ehrlich et al. ¹¹ reported the results of gene expression analyses in cultured human bronchial cells infected with SARS-CoV-2 and lung tissue from patients with COVID-19, demonstrating a marked shift in cellular metabolism and excessive intracellular lipid generation in infected cells. In this report, the transcriptional response to SARS-CoV-2 involved predominantly metabolic genes and was characterized by changes in

pathways of endoplasmic reticulum stress, upregulation of glycolysis and dysregulation of the citric acid cycle, upregulation of fatty acid and cholesterol synthesis, and the suppression of fatty acid oxidation. In further cell culture experiments, fenofibrate was reported to reverse the metabolic changes induced by SARS-CoV-2, and inhibited viral production/replication ¹¹. Interestingly, despite the potential impact of PPAR- α activation on cell metabolism in infected cells, Davies et al. reported that the PPAR- α antagonist GW6471 did not appreciably alter the antiviral actions of fenofibrate in one of their cell culture systems ¹², suggesting that the antiviral activity of fenofibrate measured in their assays was not mediated by this transcription factor. In addition to its potential antiviral activity, fenofibrate may exert immunomodulatory effects that could have an impact in COVID-19 (refs. ^{13–15}).

Despite the potential effects of fenofibrate on SARS-CoV-2 reported using in vitro culture systems, our randomized trial convincingly demonstrates the absence of an appreciable clinical benefit on all endpoints studied. There was near complete overlap between the two trial arms in our primary endpoint, which incorporates multiple clinically relevant aspects of COVID-19 severity. Similarly, there was

no benefit of fenofibrate on multiple prespecified secondary and exploratory endpoints, as well as in sensitivity analyses and in various prespecified subgroup analyses. The clear lack of a clinical benefit in our double-blinded, randomized trial contrasts with the various *in vitro* effects reported as detailed above. Importantly, the pathogenesis of COVID-19 is complex and involves not only primary cytotoxic effects of SARS-CoV-2 but also a complex set of systemic host responses that involve the innate and acquired immune systems, various neurohormonal canonical pathways, as well as multi-organ damage and failure^{20–22}. Therefore, *in vitro* cellular effects of drugs may fail to translate into clinical benefit as a result of a wide host of potential pathophysiological phenomena in whole organisms. Our trial reinforces the importance of not equating *in vitro* efficacy against SARS-CoV-2 with clinical efficacy in the setting of COVID-19, and further demonstrates the importance of performing rigorous prospective randomized controlled trials to assess the potential clinical benefit of interventions for COVID-19 before clinical implementation.

Our study also provides important safety data for this widely available medication. Although a trend towards a higher incidence of gastrointestinal side effects was observed, our trial demonstrates that fenofibrate therapy was not associated with an excess of major adverse events. These findings suggest that this medication can be safely administered or continued in patients with COVID-19 who require it for other indications, such as dyslipidaemia.

Our study is strengthened by the use of a double-blinded, placebo-controlled, randomized study design, which overcomes the problem of confounding due to multiple known or unknown uncontrolled factors, as occurs in observational studies. We enrolled participants across multiple international centres with diverse, global representation of individuals affected by COVID-19. Participants were recruited as both inpatients and outpatients from medical centres in diverse settings, using a pragmatic approach to capture data collected during routine care, further contributing to generalizability of the results to a broad population of those susceptible to COVID-19. There were low rates of attrition of study participants and high rates of adherence to the study medication, which were similar across the randomization arms. The use of the ranked severity score as the primary endpoint incorporated several clinical events highly relevant to patients with COVID-19 into a single outcome measure. Our relatively large sample size further facilitated evaluation for clinically meaningful differences in several secondary endpoints. There are also notable limitations. The study enrolled participants over an 18-month period during which there were several different dominant SARS-CoV-2 variants and management strategies as well as the introduction of vaccines, all of which varied across countries at different timepoints. While vaccination status was balanced across treatment arms, we were not able to collect information on which SARS-CoV-2 variants participants were infected with. We attempted to address this by adjusting for country and epoch (that is, time since trial initiation) and clustering by study site in secondary analyses to account for differences in treatment practices over time and by location. These adjustments did not appreciably impact our findings. We also performed subgroup analyses, which demonstrated no meaningful differences across locations and epochs. Finally, limitations of our hierarchical primary endpoint should be considered. Given that the clinical presentation and course of COVID-19 is highly variable, the design of a clinical trial endpoint that provides clinically meaningful results in patients across the spectrum of illness represents an important challenge in the field. Whereas our hierarchical endpoint has various advantages as mentioned above, it also has disadvantages. First, each of the components of the endpoint may be considered more or less important, and such assigned importance may in turn be affected by specific clinical, public health and societal circumstances at a given time, as well as by individual patient wishes. Moreover, even if the circumstances mentioned above are not considered, the hierarchical endpoint could provide results

that are not straightforward to interpret from a clinical standpoint. In particular, a given significant difference in the endpoint between the arms may not intuitively represent the magnitude of the achieved clinical benefit in daily practice. Nevertheless, in our case, the clearly neutral results obtained with the primary endpoint, as well as with all secondary and exploratory endpoints, provide us with an overall high level of confidence in our conclusion regarding the lack of substantial clinical efficacy of fenofibrate among patients with COVID-19 with clinical characteristics corresponding to our inclusion/exclusion criteria.

In conclusion, in our multicentre, randomized, placebo-controlled trial, fenofibrate did not exert any appreciable clinical benefits among patients with COVID-19. Further studies are required to assess whether various other interventions designed to affect cellular metabolic pathways can impact clinical outcomes in COVID-19.

Methods

Study design and oversight

The FERMIN trial was a prospective, multicentre, randomized, double-blinded trial conducted at 25 centres in 6 countries (United States, Mexico, Greece, Peru, Colombia and Lebanon). The study protocol for this clinical trial (ClinicalTrials.gov registration no. [NCT04517396](#)) is available in the Supplementary Information. A data coordinating centre at the University of Pennsylvania oversaw data management and statistical analyses. The trial design was approved by the ethics committee of each participating centre, including the institutional review board of the Perelman School of Medicine at the University of Pennsylvania (which also oversaw activities at the University of Arizona via reliance agreements), the Peruvian National Transitory Committee of Research Ethics for the Evaluation and Supervision of Clinical Trials in COVID-19 (IETSI, Lima, Peru), the National Ethics Committee of Greece (Athens, Greece), The Institutional Review Committee and Independent Committee of Research Ethics at CIRCIE-BIOMELAB (Barranquilla, Colombia), the Research Ethics Committee at CEI FOSCAL (Santander, Colombia), the Research Ethics Committee at Fundación del Caribe Para la Investigación Biomédica (Fundación BIOS; Barranquilla, Colombia), the Regional Clinical Research Ethics Committee at Clínica del Eje Cafetero (Manizales, Colombia), the Research Ethics Committee at Clínica de Marly S.A. (Bogota, Colombia), the Institutional Review board at American University of Beirut (Beirut, Lebanon), the Makassed General Hospital Institutional Review Board (Beirut, Lebanon) and the Research Ethics Committee at Hospital Civil de Guadalajara (Guadalajara, Mexico). An independent data safety monitoring board was also assembled to provide oversight of the trial (J. Younger, ArgoPond; S. Virani, Baylor College of Medicine; M. Campos, University of Miami Miller School of Medicine; G. Heresi, Cleveland Clinic; and T. A. Miano, University of Pennsylvania Perelman School of Medicine). All participants provided written or electronic informed consent. Participants did not receive monetary compensation for their participation in the trial.

Participants

Participants who were being evaluated in emergency departments, outpatient clinics or other urgent/emergent care settings or who were admitted to the hospital with COVID-19, were assessed for eligibility.

Participants were required to: (1) be a minimum of 18 years of age; (2) carry a diagnosis of COVID-19, based on: (a) a compatible clinical presentation with a positive laboratory test for SARS-CoV-2, or (b) consideration by the primary team as a Person Under Investigation undergoing testing for COVID-19 with a high clinical probability, in addition to compatible pulmonary infiltrates on chest X-ray (bilateral, interstitial or ground glass opacities) or chest computed tomography; (3) have fewer than 14 d since symptom onset; (4) be able to provide informed consent.

Exclusion criteria were as follows: (1) known pregnancy or breastfeeding; (2) eGFR < 30 ml min⁻¹ per 1.73 m² or undergoing dialysis (chronic kidney disease stages 4–5); given the lack of available

preparations for participants with eGFR < 60 ml min⁻¹ per 1.73 m² in trial countries other than the United States (Supplementary Information), the latter eGFR cut-off point was implemented for exclusion in those countries; (3) history of active liver disease, cholelithiasis, uncontrolled hypothyroidism or rhabdomyolysis (suspected or confirmed); (4) known hypersensitivity to fenofibrate or fenofibric acid; (5) ongoing treatment with fenofibrate, clofibrate, warfarin and other coumarin anticoagulants, glimepiride, cyclosporine, tacrolimus; (6) use of statins other than simvastatin, pravastatin or atorvastatin ≤40 mg/d or rosuvastatin ≤20 mg/d; (7) prisoners/incarcerated individuals; (8) inability to read, write or no access to a smart phone, computer or tablet device (at sites where electronic informed consent was performed to minimize risk of COVID-19 exposure to study staff); (9) and intubated patients.

Randomization, blinding and treatment allocation

Eligible participants were randomized at a ratio of 1:1 to either: (1) fenofibrate (or its active metabolite, fenofibric acid) administered for 10 d by mouth^{23,24}, with appropriate dose reductions or exclusions implemented for patients with chronic kidney disease according to the approved preparation label; or (2) placebo of similar appearance. These interventions were added to usual care. Participants and investigators were blinded to the randomized intervention. Treatment allocation was concealed using a secure web-based randomization system. Permuted block randomization was performed in randomly varying block sizes by clinical site, sex, age group (<65 or ≥65 years) and inpatient versus outpatient status. All investigators collecting information on clinical endpoints were blinded to the study intervention. The specific drug preparations used in various countries are detailed in the Supplementary Information.

Criteria for study medication discontinuation included any of the following occurring at any time during the administration period: (1) acute kidney injury with an eGFR < 30 ml min⁻¹ per m²; (2) suspected or confirmed rhabdomyolysis; (3) red or brown urine, which may indicate myoglobinuria, unless considered by the investigator to be clearly not due to rhabdomyolysis (for instance, in the presence of normal circulating creatine kinase); and (4) liver failure or increased liver enzymes AST or ALT to >3 times the upper limit of normal. In cases in which the medication was discontinued, data collection continued normally according to the usual study protocol.

Follow-up and outcomes

The 'on study' period was 30 d. For participants randomized as inpatients, daily assessments (via medical record review) were performed to assess clinical status, with particular attention to the study endpoints (death, mechanical ventilation and FiO₂/SpO₂ ratio), until hospital discharge or 30 d (whichever was shortest). For participants discharged before 30 d after randomization, a follow-up call at the -30-d timepoint assessed vital and functional status, symptoms and major adverse events, including hospitalizations. For participants randomized as outpatients or discharged within 24 h of receiving the first dose of the study medication, participants were called at -5, 10, 15 and 30 d after randomization, to assess vital and functional status, hospitalization status, the severity of dyspnoea (via the modified dyspnoea Borg scale) and major adverse events.

Primary endpoint

The primary endpoint of the trial (Fig. 4) was a global severity score that hierarchically ranked participant outcomes according to five factors: (1) time to death (ranked from shortest to longest, up to 30 d after randomization); (2) the number of days supported by mechanical ventilation (invasive or noninvasive) or ECMO (until hospital discharge, up to 30 d after randomization, ranked from longest to shortest); (3) the FiO₂/SpO₂ ratio area under the curve (until hospital discharge, up to 30 d after randomization, ranked from highest to lowest); (4) for participants enrolled as outpatients who were subsequently hospitalized,

the number of days out of the hospital during the 30 d period following randomization (ranked from lowest to highest); and (5) for participants enrolled as outpatients who did not get hospitalized during the 30 d observation period, the modified dyspnoea Borg scale (mean value of assessments at -5, -10 and -15 d). Patients who were enrolled as inpatients and discharged within 24 h of receiving the first dose of the study medication were ranked similarly to outpatients. (*Hospital-based data collection for these endpoints occurs until discharge or the end of the 30-day observation period (whichever is shortest)).

The ranked severity score has several advantages compared to binary outcomes (for example, all-cause death) or time-to-event outcomes (for example, time to death)^{25–27}. It incorporates information about each of the highest-priority events in COVID-19, but allows these events to be prioritized within a single endpoint. For instance, the principal outcome of interest is death, but even if there is no difference in rate of death, we would still be interested in a shorter duration of invasive respiratory support, a shorter duration of hospital admission with better oxygenation parameters, and so on. This is aimed at maximizing study power and minimizing the number of participants that need to be enrolled to detect clinically meaningful differences.

Secondary and exploratory endpoints

Secondary endpoints were: (1) the number of days alive, out of the ICU, free of mechanical ventilation (invasive and noninvasive), ECMO or maximal available respiratory support in the 30 d following randomization; (2) a seven-category ordinal scale consisting of the following categories: not hospitalized with resumption of normal activities; not hospitalized, but unable to resume normal activities; hospitalized, not requiring supplemental oxygen; hospitalized, requiring supplemental oxygen; hospitalized, requiring nasal high-flow oxygen therapy, noninvasive mechanical ventilation, or both; hospitalized, requiring ECMO, invasive mechanical ventilation, or both; and, death; (3) a ranked severity score similar to the primary endpoint, but using a more comprehensive COVID-19 symptom scale instead of the dyspnoea Borg scale (Supplementary Appendices).

Exploratory endpoints included: (1) time to all-cause death; (2) time to hospitalization (among participants enrolled as outpatients); (3) time to discharge (among participants enrolled as inpatients); (4) the number of days alive and out of the hospital during the 30 d following randomization; (5) a ranked severity score similar to the primary endpoint, but built only with factors 1–4.

Statistical analyses

Analyses were performed on an intention-to-treat basis. The primary analyses used the non-parametric two-sided Wilcoxon rank-sum test to compare the distribution of severity scores across treatment arms. In a prespecified, secondary analysis of the primary endpoint, we used linear regression to compare mean ranked severity scores between arms after adjustment for age, sex, inpatient versus outpatient status at enrolment, FiO₂/SpO₂ ratio at the time of enrolment, race, ethnicity, BMI, history of diabetes at baseline^{1–4} and country (to account for differences in treatment practices, timing of variants, and timing of surges), with random slope and intercept to account for clustering by site. For the linear regression analyses, severity scores were condensed by level of the hierarchical outcome for clarity of interpretation of the coefficient (that is, those ranked by time to death have a score between 0 and 1; those ranked by duration of mechanical ventilation have a score between 1 and 2; those ranked by FiO₂/SpO₂ ratio have a score between 2 and 3, and so on). We evaluated time-to-event outcomes using Cox proportional hazards models from the time of enrolment and censored at the end of the 30-d follow-up period. We assessed for violation of the proportional hazards assumption using Schoenfeld residuals and planned to incorporate a time-by-treatment interaction term if the assumption was violated. In analyses that did not include death as part

of the time-to-event outcome, we evaluated cause-specific hazards to address death as a competing risk.

We performed prespecified exploratory subgroup analyses according to sex, age (categorized by < or ≥ the median value in the study population), race, presence of preexisting diabetes, BMI (categorized by ≥30 or <30 kg/m²), inpatient versus outpatient status at the time of enrolment, FiO₂/SpO₂ ratio at the time of enrolment (categorized by < or ≥ the median value in the study population), duration of symptoms before randomization (<7 versus ≥7 d), country, baseline COVID-19 severity based on the WHO criteria²⁸ and fenofibrate formulation, using the two-sided van Elteren test to compare severity scores stratified by these prespecified subgroups^{29,30}.

The analysis was based on complete cases, and ignored missing data. This approach was prespecified based on a missingness rate of less than 5% (Supplementary Methods). The two-sided type I error rate was 0.05 and was not adjusted for multiple comparisons except for the primary analysis, which included an interim analysis; CIs were at the 95% level. Analyses were performed using Stata version 16.1 (StataCorp).

Power calculation

Using Monte Carlo simulations to apply likely distributions of participants across each of the hierarchies based on available published data^{31,32}, we estimated that the trial would have 80% power at an alpha value of 0.0492 (allowing for one interim analysis at 50% of enrolment with an alpha value of 0.0054 (refs. ^{33,34}) to demonstrate an 11% difference in median ranked severity scores between the treatment arms at the target sample size of 700. Power calculations were performed using Python and PASS 16 software³⁵. Power calculations for other endpoints are presented in the Supplementary Information.

Protocol deviations

One participant continued to receive the study medication for 3 d after developing acute kidney injury with an eGFR < 30 ml min⁻¹ per 1.73 m², which was an indication for early termination of the study medication according to the protocol. Two participants were enrolled who unknowingly had exclusion criteria at the time of enrolment (one had a previous history of cholecystectomy and the other had hypothyroidism); both participants were withdrawn from the study as soon as the study team became aware of these elements of the medical history. One participant did not receive trial medication while hospitalized on one day because the medication could not be located by the nurse on the unit and the study team was not made aware until the following day, when it was re-administered. One participant's 15-d symptom call was not performed within the permitted time frame due to an oversight of the study team. Six participants in Peru did not have transaminase determinations performed either at baseline or 5 d after enrolment as required by the study protocol for safety monitoring in that country. Two witnesses of the informed consent entered the incorrect document identification number at the time of consenting; the participants were subsequently re-consented. Three participants initially signed the wrong version of the consent form and were subsequently re-consented using the correct version.

Reporting summary

Further information on research design is available in the Nature Portfolio Reporting Summary linked to this article.

Data availability

The trial data are not publicly available but may be made available for scientific collaborations after the execution of appropriate data sharing agreements, after review and approval of requests by the trial data coordinating centre and enrolment site investigators, as allowed by existing local/national regulations and data sharing agreements with each centre.

References

- Bornstein, S. R., Dalan, R., Hopkins, D., Migrone, G. & Boehm, B. O. Endocrine and metabolic link to coronavirus infection. *Nat. Rev. Endocrinol.* **16**, 297–298 (2020).
- Zhou, F. et al. Clinical course and risk factors for mortality of adult inpatients with COVID-19 in Wuhan, China: a retrospective cohort study. *Lancet* **395**, 1054–1062 (2020).
- Guan, W. J. et al. Clinical characteristics of coronavirus disease 2019 in China. *N. Engl. J. Med.* **382**, 1708–1720 (2020).
- Wu, C. et al. Risk factors associated with acute respiratory distress syndrome and death in patients with coronavirus disease 2019 pneumonia in Wuhan, China. *JAMA Intern. Med.* **180**, 934–943 (2020).
- Oguz, S. H. & Okan Yildiz, B. Endocrine disorders and COVID-19. *Annu. Rev. Med.* <https://doi.org/10.1146/annurev-med-043021-033509> (2022).
- Vassilopoulou, E., Bumbacea, R. S., Pappa, A. K., Papadopoulos, A. N. & Bumbacea, D. Obesity and infection: what have we learned from the COVID-19 pandemic. *Front Nutr.* **9**, 931313 (2022).
- Zhu, L. et al. Association of blood glucose control and outcomes in patients with COVID-19 and preexisting type 2 diabetes. *Cell Metab.* **31**, 1068–1077 (2020).
- Wu, Z. et al. Palmitoylation of SARS-CoV-2 S protein is essential for viral infectivity. *Signal Transduct. Target Ther.* **6**, 231 (2021).
- Li, D., Liu, Y., Lu, Y., Gao, S. & Zhang, L. Palmitoylation of SARS-CoV-2 S protein is critical for S-mediated syncytia formation and virus entry. *J. Med Virol.* **94**, 342–348 (2022).
- Nguyen, H. T. et al. Spike glycoprotein and host cell determinants of SARS-CoV-2 entry and cytopathic effects. *J. Virol.* **95**, e02304–20 (2020).
- Ehrlich, E. et al. The SARS-CoV-2 transcriptional metabolic signature in lung epithelium. *SSRN Journal* <https://doi.org/10.2139/ssrn.3650499> (2020).
- Davies, S. P. et al. The hyperlipidaemic drug fenofibrate significantly reduces infection by SARS-CoV-2 in cell culture models. *Front. Pharm.* **12**, 660490 (2021).
- Schaefer, M. B. et al. Peroxisome proliferator-activated receptor-alpha reduces inflammation and vascular leakage in a murine model of acute lung injury. *Eur. Respir. J.* **32**, 1344–1353 (2008).
- Hecker, M. et al. PPAR-α activation reduced LPS-induced inflammation in alveolar epithelial cells. *Exp. Lung Res.* **41**, 393–403 (2015).
- Huang, D., Zhao, Q., Liu, H., Guo, Y. & Xu, H. PPAR-α agonist WY-14643 inhibits LPS-induced inflammation in synovial fibroblasts via NF-κB pathway. *J. Mol. Neurosci.* **59**, 544–553 (2016).
- Nardacci, R. et al. Evidences for lipid involvement in SARS-CoV-2 cytopathogenesis. *Cell Death Dis.* **12**, 263 (2021).
- Sagan, S. M. et al. The influence of cholesterol and lipid metabolism on host cell structure and hepatitis C virus replication. *Biochem. Cell Biol.* **84**, 67–79 (2006).
- Dorobantu, C. M. et al. Modulation of the host lipid landscape to promote RNA virus replication: the picornavirus encephalomyocarditis virus converges on the pathway used by hepatitis C virus. *PLoS Pathog.* **11**, e1005185 (2015).
- Yan, B. et al. Characterization of the lipidomic profile of human coronavirus-infected cells: implications for lipid metabolism remodeling upon coronavirus replication. *Viruses* <https://doi.org/10.3390/v11010073> (2019).
- Lamers, M. M. & Haagmans, B. L. SARS-CoV-2 pathogenesis. *Nat. Rev. Microbiol.* **20**, 270–284 (2022).
- Alipoor, S. D. et al. COVID-19: molecular and cellular response. *Front. Cell Infect. Microbiol.* **11**, 563085 (2021).

22. Wiersinga, W. J., Rhodes, A., Cheng, A. C., Peacock, S. J. & Prescott, H. C. Pathophysiology, transmission, diagnosis and treatment of coronavirus disease 2019 (COVID-19): a review. *JAMA* **324**, 782–793 (2020).
23. Ling, H., Luoma, J. T. & Hilleman, D. A review of currently available fenofibrate and fenofibric acid formulations. *Cardiol. Res.* **4**, 47–55 (2013).
24. Ladabaum, U., Mammalithara, A., Myer, P. A. & Singh, G. Obesity, abdominal obesity, physical activity, and caloric intake in US adults: 1988 to 2010. *Am. J. Med* **127**, 717–727 (2014).
25. O'Connor, C. M. et al. Cardiovascular outcomes with minute ventilation-targeted adaptive servo-ventilation therapy in heart failure: the CAT-HF trial. *J. Am. Coll. Cardiol.* **69**, 1577–1587 (2017).
26. Margulies, K. B. et al. Effects of liraglutide on clinical stability among patients with advanced heart failure and reduced ejection fraction: a randomized clinical trial. *JAMA* **316**, 500–508 (2016).
27. Felker, G. M. & Maisel, A. S. A global rank end point for clinical trials in acute heart failure. *Circ. Heart Fail.* **3**, 643–646 (2010).
28. World Health Organization. R&D Blueprint: novel coronavirus. COVID-19 therapeutic trial synopsis draft. 18 February 2020. https://www.who.int/blueprint/priority-diseases/key-action/COVID-19_Treatment_Trial_Design_Master_Protocol_synopsis_Final_18022020.pdf. Accessed 28 April 2020.
29. van Elteren, P. H. On the combination of independent two sample tests of Wilcoxon. *Bull. Int. Stat. Inst.* **37**, 351–361 (1960).
30. Fay, M. P. & Malinovsky, Y. Confidence intervals of the Mann-Whitney parameter that are compatible with the Wilcoxon Mann-Whitney test. *Stat. Med.* **37**, 3991–4006 (2018).
31. Wang, D. et al. Clinical characteristics of 138 hospitalized patients with 2019 novel coronavirus-infected pneumonia in Wuhan, China. *JAMA* **323**, 1061–1069 (2020).
32. Hozo, S. P., Djulbegovic, B. & Hozo, I. Estimating the mean and variance from the median, range, and the size of a sample. *BMC Med. Res. Methodol.* **5**, 13 (2005).
33. Julious, S. A. Tutorial in biostatistics. Sample sizes for clinical trials with normal data. *Stat. Med.* **23**, 1921–1986 (2004).
34. O'Brien, P. C. & Fleming, T. R. A multiple testing procedure for clinical trials. *Biometrics* **35**, 549–556 (1979).
35. PASS 16 Power Analysis and Sample Size software. NCSS, LLC. Kaysville, Utah, USA. <https://www.ncss.com/software/pass/>. (2018).

Acknowledgements

This trial was funded by NCATS grant 1U01TR003734-01 and by an investigator-initiated grant from Abbott Laboratories to the University of Pennsylvania. The sponsors had no role in study design, clinical data collection, outcome adjudication or data analysis. The authors would like to thank the members of the Data Safety Monitoring Board for their oversight of the trial: J. Younger, S. Virani, G. Heresi, M. Campos and T. Miano. We also thank B. A. Mount and C. Colvis, Program Officers of the National Center for Advancing Translational Sciences, for their support. The authors also thank the following individuals for their invaluable contributions to the trial: C. Magro, E. Chau, E. Moriarty, A. Novotny, A. Gowda, H. Maynard, M. del Portal, M. López-Pico, T. Valencia, O. L. Bello, A. L. Perez and A. Valenzuela-Ramírez. The investigators are also grateful to Abbott Product Operations AG, particularly J.-P. Berrou, A. Virkar, C. Braganza and A. Rojas for their support in providing investigational product and placebo for various study sites.

Author contributions

J.A.C. provided conception and design of the work, acquisition and interpretation of data, drafting and revision of the manuscript, supervision of the overall trial. J.B.C. provided design of the work; acquisition, analysis, and interpretation of data; drafting and revision

of the manuscript. J.C. and M.P. provided analysis and interpretation of the data. P.L.-J., E.J.G.-B., G.H.D.d.C., A.R.B., J.F.A.-V., O.S., C.C.-C., N.R.R.-S., M.P.C.G., L.A.G.-H., R.M., R.A., M.E.C.S., M.P., C.M., I.D., C.V., C.G., J.E.R.-M., E.G.-L., R.C.P., J.L.R.H., H.A., J.A.-M., M.P.-M., C.M., G.P., G.S., R.V.-V., M.V.-C., R.J.A.-G., C.A.C.-C., R.M.A.C., W.G.L.D., T.S., K.G., B.P., C.G., J.O.-L., D.J., P.K., Z.A., S.S., N.K.S., C.B.A., D.M.M.S., E.F.B.S., C.J.C.D., U.M.V.G., C.D.S.H., N.L.B.T., J.C.C.G., E.M.V., P.W., H.E.-R., I.R.B.-F. and P.A.S.-S. provided acquisition of the data and critical revision of the manuscript. All authors approved of the final version of the manuscript.

Competing interests

In the last 2 years, J.B.C. has received research grants from the National Institutes of Health and American Heart Association. In the last 2 years, J.A.C. has received consulting honoraria from Sanifit, Bristol Myers Squibb, Merck, Edwards Lifesciences, Bayer, JNJ, the University of Delaware, and research grants from the National Institutes of Health, Abbott, Microsoft, Fukuda-Denshi and Bristol Myers Squibb. J.A.C. has received compensation from the American Heart Association and the American College of Cardiology for editorial roles, and visiting speaker honoraria from Washington University, University of Utah, the Japanese Association for Cardiovascular Nursing and the Korean Society of Cardiology. E.J.G. has received honoraria from Abbott CH, bioMérieux, Brahms, GSK, InflaRx, Sobi and XBiotech; independent educational grants from Abbott CH, AxisShield, bioMérieux, InflaRx, Johnson & Johnson, MSD, Sobi and XBiotech; and funding from the Horizon 2020 Marie-Curie Project European Sepsis Academy (granted to the National and Kapodistrian University of Athens), and the Horizon 2020 European Grants ImmunoSep and RISKinCOVID (granted to the Hellenic Institute for the Study of Sepsis). In the last 2 years, N.K.S. has received compensation from the American Heart Association for editorial duties. The remaining authors declare no competing interests.

Additional information

Extended data is available for this paper at <https://doi.org/10.1038/s42255-022-00698-3>.

Supplementary information The online version contains supplementary material available at <https://doi.org/10.1038/s42255-022-00698-3>.

Correspondence and requests for materials should be addressed to Julio A. Chirinos.

Peer review information *Nature Metabolism* thanks Charlotte Steenblock, Daniel Clark Files and the other, anonymous, reviewer(s) for their contribution to the peer review of this work. Primary Handling Editors: Ashley Castellanos-Jankiewicz and Christoph Schmitt, in collaboration with the *Nature Metabolism* team.

Reprints and permissions information is available at www.nature.com/reprints.

Publisher's note Springer Nature remains neutral with regard to jurisdictional claims in published maps and institutional affiliations.

Springer Nature or its licensor (e.g. a society or other partner) holds exclusive rights to this article under a publishing agreement with the author(s) or other rightsholder(s); author self-archiving of the accepted manuscript version of this article is solely governed by the terms of such publishing agreement and applicable law.

© The Author(s), under exclusive licence to Springer Nature Limited 2022

Julio A. Chirinos¹✉, Patricio Lopez-Jaramillo², Evangelos J. Giamarellos-Bourboulis³, Gonzalo H. Dávila-del-Carpio¹⁴, Abdul Rahman Bizri⁵, Jaime F. Andrade-Villanueva¹⁶, Oday Salman³⁵, Carlos Cure-Cure⁷, Nelson R. Rosado-Santander⁸, Mario P. Cornejo Giraldo¹⁹, Luz A. González-Hernández⁶, Rima Moghnieh¹⁰, Rapti Angeliki¹¹, María E. Cruz Saldarriaga¹², Marcos Pariona¹¹³, Carola Medina¹³, Ioannis Dimitroulis¹¹¹, Charalambos Vlachopoulos¹⁴, Corina Gutierrez⁷, Juan E. Rodriguez-Mori¹¹⁵, Edgar Gomez-Laiton¹¹⁶, Rosa Cotrina Pereyra¹⁷, Jorge Luis Ravelo Hernández¹⁸, Hugo Arbañil¹⁹, José Accini-Mendoza²⁰, Maritza Pérez-Mayorga²¹, Charalampos Milionis¹²², Garyfallia Poulakou²³, Gregorio Sánchez²⁴, Renzo Valdivia-Vega¹¹³, Mirko Villavicencio-Carranza¹³, Ricardo J. Ayala-García¹¹³, Carlos A. Castro-Callirgos¹⁵, Rosa M. Alfaro Carrasco, Willy Garrido Lecca Danos, Tiffany Sharkoski³, Katherine Greene³, Bianca Pourmussa³, Candy Greczylo³, Juan Ortega-Legaspi³, Douglas Jacoby³, Jesse Chittams²⁵, Paraskevi Katsaounou²⁶, Zoi Alexiou²⁷, Styliani Sympardi²⁸, Nancy K. Sweitzer^{29,30}, Mary Putt³¹, Jordana B. Cohen^{31,32} & the FERMIN Investigators*

¹Division of Cardiovascular Medicine, Perelman School of Medicine, University of Pennsylvania, Philadelphia, PA, USA. ²Instituto de Investigación MASIRA, Facultad de Ciencias de la Salud, Universidad de Santander, Bucaramanga, Colombia. ³4th Department of Internal Medicine, National and Kapodistrian University of Athens, Medical School and Hellenic Institute for the Study of Sepsis, Athens, Greece. ⁴Universidad Católica de Santa María, Arequipa, Peru.

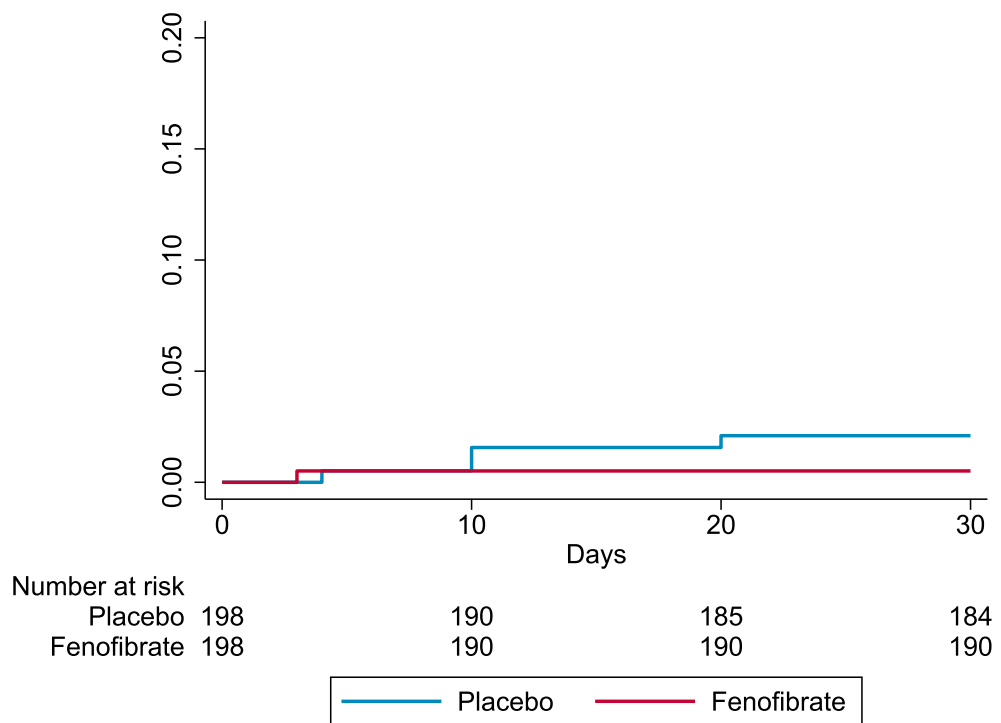
⁵Department of Medicine, American University of Beirut, Beirut, Lebanon. ⁶Unidad de VIH, Hospital Civil de Guadalajara and Universidad de Guadalajara, Guadalajara, Mexico. ⁷BIOMELAB S.A.S., Barranquilla, Colombia. ⁸Department of Medicine, Hospital Nacional Carlos Alberto Seguín Escobedo, EsSalud, Arequipa, Peru. ⁹Hospital Carlos Alberto Seguín Escobedo, Arequipa, Peru. ¹⁰Department of Medicine, Makassed General Hospital, Beirut, Lebanon. ¹¹6th Department of Pulmonary Medicine, SOTIRIA Athens General Hospital of Chest Disease, Athens, Greece. ¹²Centro de Investigación de Enfermedades Infecciosas y Tropicales, Hospital Nacional Adolfo Guevara Velasco, Cuzco, Peru. ¹³Hospital Nacional Edgardo Rebagliati Martins, EsSalud, Lima, Peru.

¹⁴1st Department of Cardiology, National and Kapodistrian University of Athens, Medical School, Athens, Greece. ¹⁵Department of Nephrology, Hospital Nacional Alberto Sabogal Sologuren, EsSalud, Lima, Peru. ¹⁶FOSCAL Internacional Floridablanca, Santander, Colombia. ¹⁷Hospital Nacional Guillermo Almenara Irigoyen, Lima, Peru. ¹⁸Hospital Central Fuerza Aérea del Peru, Miraflores, Peru. ¹⁹Hospital Nacional Dos de Mayo, Lima, Peru. ²⁰IPS Centro Científico Asistencial, Barranquilla, Colombia. ²¹Clinica de Marly, Sede UNIMARLY, Bogota, Colombia. ²²Department of Internal Medicine, Ioannina University General Hospital, Ioannina, Greece. ²³3rd Department of Internal Medicine, National and Kapodistrian University of Athens, Medical School, Athens, Greece. ²⁴Fundación Cardiomet Cequin, Armenia, Colombia. ²⁵Biostatistics Analysis Core, Office of Nursing Research, University of Pennsylvania School of Nursing, Philadelphia, PA, USA. ²⁶Section of Pneumonology and Respiratory Failure, 1st Department of Critical Care Medicine, National and Kapodistrian University of Athens, Medical School, Athens, Greece. ²⁷2nd Department of Internal Medicine, THRIASIO Eleusis General Hospital, Eleusis, Greece. ²⁸1st Department of Internal Medicine, THRIASIO Eleusis General Hospital, Eleusis, Greece. ²⁹Department of Medicine, Washington University School of Medicine, St. Louis, MO, USA. ³⁰Division of Cardiology, University of Arizona, Tucson, AZ, USA. ³¹Department of Biostatistics, Epidemiology & Informatics, Perelman School of Medicine, University of Pennsylvania, Philadelphia, PA, USA. ³²Renal-Electrolyte and Hypertension Division, Perelman School of Medicine, University of Pennsylvania, Philadelphia, PA, USA. *A list of authors and their affiliations appears at the end of the paper.

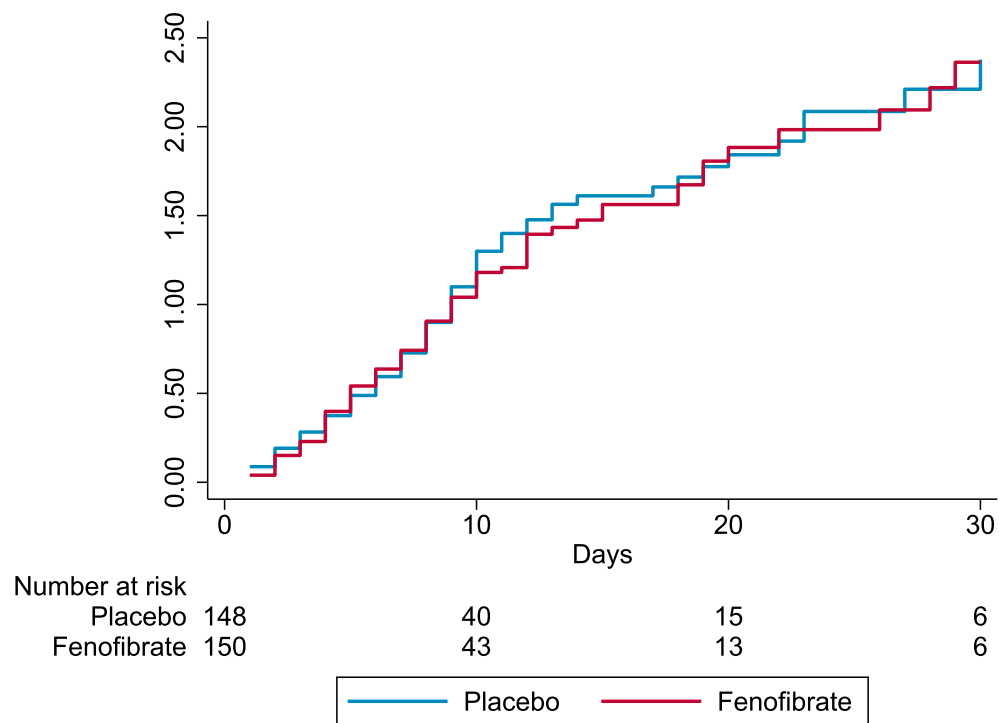
✉ e-mail: julio.chirinos@uphs.upenn.edu

the FERMIN Investigators

Ciro Barrantes Alarcón¹⁷, Denisse Marylyn Mendoza Sanchez¹⁹, Eduardo Francisco Bernales Salas⁸, Claudia Jesús Chamby Díaz⁸, Ursula Milagros Vargas Gómez⁸, Cynthia Daniela Salinas Herrera⁸, Naldy Lidia Barriga Triviños⁸, Johanna Carolina Coacalla Guerra⁸, Evelyn Marrón Veria⁸, Preethi William³⁰, Hugo Espinoza-Rojas¹³, Irving Renato Benites-Flores¹³ & Pedro Antonio Segura-Saldaña¹³



Extended Data Fig. 1 | Kaplan–Meier curve of time to hospitalization (among participants enrolled as outpatients).



Extended Data Fig. 2 | Cumulative incidence curve of time to discharge (among participants enrolled as inpatients).

Extended Data Table 1 | Components of the global rank score by study arm

<i>Variable</i>		<i>Total</i> (n=701)	<i>Placebo</i> (n=350)	<i>Fenofibrate</i> (n=351)
Death	N (%)	41 (6%)	22 (6%)	19 (5%)
Time to death, days	Mean (SD)	13 (8)	12 (9)	13 (6)
Invasive mechanical ventilation/ECMO*	N (%)	46 (7%)	27 (8%)	19 (5%)
Duration of mechanical ventilation/ECMO, days*	Mean (SD)	15 (11)	15 (10)	16 (11)
FiO ₂ /SpO ₂ †	Mean (SD)	0.19 (0.49)	0.19 (0.48)	0.18 (0.49)
Hospitalization†	N (%)	5 (1%)	4 (1%)	1 (<1%)
Duration of hospitalization, days†	Mean (SD)	9 (6)	10 (7)	5 (N/A)
Borg score during follow-up†	Mean (SD)	0.6 (1.2)	0.5 (1.1)	0.6 (1.3)
Pooled COVID-19 symptom score during follow-up†	Mean (SD)	7 (9)	7 (9)	8 (10)

Extended Data Table 2 | Adverse events by study arm

<i>Variable</i>	<i>Total</i> (n=701)	<i>Placebo</i> (n=350)	<i>Fenofibrate</i> (n=351)
Serious AEs	107 (15%)	61 (17%)	46 (13%)
Death	41 (6%)	22 (6%)	19 (5%)
Kidney	37 (5%)	22 (6%)	15 (4%)
Hepatic	48 (7%)	25 (7%)	23 (7%)
Cardiovascular	26 (4%)	12 (3%)	14 (4%)
Respiratory	76 (11%)	41 (12%)	35 (10%)
Gastroenterologic	28 (4%)	9 (3%)	19 (5%)
Infectious	55 (8%)	25 (7%)	30 (9%)
Intensive care unit transfer	29 (4%)	16 (5%)	13 (4%)
Delirium	9 (1%)	3 (<1%)	6 (2%)
Neurologic	8 (1%)	4 (1%)	4 (1%)
Dermatologic	4 (<1%)	2 (<1%)	2 (<1%)
Ophthalmologic	1 (<1%)	0 (0%)	1 (<1%)
Endocrinologic	3 (<1%)	2 (<1%)	1 (<1%)
Hematologic	22 (3%)	12 (3%)	10 (3%)
Musculoskeletal	8 (1%)	4 (1%)	4 (1%)

Reporting Summary

Nature Portfolio wishes to improve the reproducibility of the work that we publish. This form provides structure for consistency and transparency in reporting. For further information on Nature Portfolio policies, see our [Editorial Policies](#) and the [Editorial Policy Checklist](#).

Statistics

For all statistical analyses, confirm that the following items are present in the figure legend, table legend, main text, or Methods section.

n/a Confirmed

- The exact sample size (n) for each experimental group/condition, given as a discrete number and unit of measurement
- A statement on whether measurements were taken from distinct samples or whether the same sample was measured repeatedly
- The statistical test(s) used AND whether they are one- or two-sided
 - Only common tests should be described solely by name; describe more complex techniques in the Methods section.*
- A description of all covariates tested
- A description of any assumptions or corrections, such as tests of normality and adjustment for multiple comparisons
- A full description of the statistical parameters including central tendency (e.g. means) or other basic estimates (e.g. regression coefficient) AND variation (e.g. standard deviation) or associated estimates of uncertainty (e.g. confidence intervals)
- For null hypothesis testing, the test statistic (e.g. F , t , r) with confidence intervals, effect sizes, degrees of freedom and P value noted
 - Give P values as exact values whenever suitable.*
- For Bayesian analysis, information on the choice of priors and Markov chain Monte Carlo settings
- For hierarchical and complex designs, identification of the appropriate level for tests and full reporting of outcomes
- Estimates of effect sizes (e.g. Cohen's d , Pearson's r), indicating how they were calculated

Our web collection on [statistics for biologists](#) contains articles on many of the points above.

Software and code

Policy information about [availability of computer code](#)

Data collection

Data was collected in REDCAP versions 11.2-12.1

Data analysis

Analyses were performed using Stata version 16.1 (StataCorp, College Station, TX)

For manuscripts utilizing custom algorithms or software that are central to the research but not yet described in published literature, software must be made available to editors and reviewers. We strongly encourage code deposition in a community repository (e.g. GitHub). See the Nature Portfolio [guidelines for submitting code & software](#) for further information.

Data

Policy information about [availability of data](#)

All manuscripts must include a [data availability statement](#). This statement should provide the following information, where applicable:

- Accession codes, unique identifiers, or web links for publicly available datasets
- A description of any restrictions on data availability
- For clinical datasets or third party data, please ensure that the statement adheres to our [policy](#)

The trial data is not publicly available but may be made available for scientific collaborations after the execution of appropriate data sharing agreements, after review and approval of requests by the trial data coordinating center and enrolment site investigators, as allowed by existing local/national regulations and data sharing agreements with each center. The corresponding author should be contacted with any data requests.

Human research participants

Policy information about [studies involving human research participants and Sex and Gender in Research](#).

Reporting on sex and gender	Only sex (self reported) was considered
Population characteristics	Shown in detail in Table 1
Recruitment	Participants were recruited as both inpatients and outpatients from medical centers in diverse settings upon presentation to the emergency room with COVID-19. Given the broad range of availability of healthcare resources and patient demographics across the sites, there is no clear systematic source of selection bias that would be expected to affect the results
Ethics oversight	Institutional IRBs, ad hoc DSMB and National regulatory entities as needed. The trial design was approved by the ethics committee of each participating center, including the institutional review board of the Perelman School of Medicine at the University of Pennsylvania (Philadelphia, PA, which also oversaw activities at the University of Arizona via reliance agreements), the Peruvian National Transitory Committee of Research Ethics for the Evaluation and Supervision of Clinical Trials in COVID-19 (IETSI, Lima, Perú), the National Ethics Committee of Greece (Athens, Greece), The Institutional Review Committee and Independent Committee of Research Ethics at CIRCIE-BIOMELAB (Barranquilla, Colombia), the Research Ethics Committee at CEI FOSCAL (Santander, Colombia), the Research Ethics Committee at Fundación del Caribe Para la Investigación Biomédica (Fundación BIOS; Barranquilla, Colombia), the Regional Clinical Research Ethics Committee at Clínica del Eje Cafetero (Manizales, Colombia), the Research Ethics Committee at Clínica de Marly S.A. (Bogotá, Colombia), the Institutional Review board at American University of Beirut (Beirut, Lebanon), the Makassed General Hospital Institutional Review Board (Beirut, Lebanon) and the Research Ethics Committee at Hospital Civil de Guadalajara (Guadalajara, Mexico).

Note that full information on the approval of the study protocol must also be provided in the manuscript.

Field-specific reporting

Please select the one below that is the best fit for your research. If you are not sure, read the appropriate sections before making your selection.

Life sciences Behavioural & social sciences Ecological, evolutionary & environmental sciences

For a reference copy of the document with all sections, see nature.com/documents/nr-reporting-summary-flat.pdf

Life sciences study design

All studies must disclose on these points even when the disclosure is negative.

Sample size	Using Monte Carlo simulations to apply likely distributions of participants across each of the hierarchies based on available published data, ^{2,29,30} we estimated that the trial would have 80% power at an alpha of 0.0492 (allowing for one interim analysis at 50% of enrollment with an alpha of 0.005431, ³²) to demonstrate an 11% difference in median ranked severity scores between the treatment arms at the target sample size of 700. Power calculations were performed using Python and PASS16. ³³ Power calculations for other endpoints are presented in the supplemental section.
Data exclusions	exclusion criteria were pre-established. No post hoc data exclusions. Exclusion criteria were as follows: (1) known pregnancy or breastfeeding; (2) estimated glomerular filtration rate (eGFR) <30 mL/min/1.73 m ² or undergoing dialysis (chronic kidney disease stages 4–5); given the lack of available preparations for participants with eGFR<60 mL/min/1.73 m ² in trial countries other than the USA (see supplemental section), the latter eGFR cut-point was implemented for exclusion in those countries; (3) history of active liver disease, cholelithiasis, uncontrolled hypothyroidism, or rhabdomyolysis (suspected or confirmed); (4) known hypersensitivity to fenofibrate or fenofibric acid; (5) ongoing treatment with fenofibrate, clofibrate, warfarin and other coumarin anticoagulants, glimepiride, cyclosporine, tacrolimus; (6) use of statins other than simvastatin, pravastatin or atorvastatin ≤40 mg/d or rosuvastatin ≤20 mg/d; (7) prisoners/incarcerated individuals; (8) inability to read, write or no access to a smart phone, computer or tablet device (at sites where eConsenting was performed to minimize risk of COVID-19 exposure to study staff); (9) intubated patients.
Replication	No replication done, as this was a randomized controlled trial in humans and replication of the trial was not feasible within a reasonable time frame and given available resources. Nonetheless, internal consistency was tested in various subgroups as per study protocol
Randomization	Eligible participants were randomized 1:1 to either: (1) fenofibrate (or its active metabolite, fenofibric acid) or (2) placebo of similar appearance. Treatment allocation was concealed using a secure web-based randomization system. Permuted block randomization was performed in randomly varying block sizes by clinical site, sex, age group (<65 or ≥65 years) and inpatient vs. outpatient status. All investigators collecting information on clinical endpoints were blinded to the study intervention.
Blinding	Participants and investigators were blinded to the randomized intervention.

Reporting for specific materials, systems and methods

We require information from authors about some types of materials, experimental systems and methods used in many studies. Here, indicate whether each material, system or method listed is relevant to your study. If you are not sure if a list item applies to your research, read the appropriate section before selecting a response.

Materials & experimental systems

n/a	Involved in the study
<input checked="" type="checkbox"/>	Antibodies
<input checked="" type="checkbox"/>	Eukaryotic cell lines
<input checked="" type="checkbox"/>	Palaeontology and archaeology
<input checked="" type="checkbox"/>	Animals and other organisms
<input type="checkbox"/>	Clinical data
<input checked="" type="checkbox"/>	Dual use research of concern

Methods

n/a	Involved in the study
<input checked="" type="checkbox"/>	ChIP-seq
<input checked="" type="checkbox"/>	Flow cytometry
<input checked="" type="checkbox"/>	MRI-based neuroimaging

Clinical data

Policy information about [clinical studies](#)

All manuscripts should comply with the [ICMJE guidelines for publication of clinical research](#) and a completed [CONSORT checklist](#) must be included with all submissions.

Clinical trial registration

NCT04517396

Study protocol

included with submission

Data collection

Participants were enrolled from October 2, 2020 to February 27, 2022 and data were collected through March 29, 2022. Participants were recruited as both inpatients and outpatients from medical centers in diverse settings, using a pragmatic approach to capture data collected in the electronic health record during routine care, in addition to participant surveys which were collected by phone or electronically via email. All data collected were recorded online via REDCap

Outcomes

Detailed description in manuscript:

The primary endpoint of the trial (Figure 4) was a global severity score that hierarchically ranked participant outcomes according to 5 factors: (1) time to death (ranked from shortest to longest, up to 30 days post-randomization), (2) the number of days supported by mechanical ventilation (invasive or non-invasive) or extracorporeal membrane oxygenation (until hospital discharge, up to 30 days post-randomization, ranked from longest to shortest); (3) the inspired concentration of oxygen/percent oxygen saturation (FiO₂/SpO₂) ratio area under the curve (until hospital discharge, up to 30 days post-randomization, ranked from highest to lowest); (4) for participants enrolled as outpatients who were subsequently hospitalized, the number of days out of the hospital during the 30-day period following randomization (ranked from lowest to highest); (5) for participants enrolled as outpatients who did not get hospitalized during the 30-day observation period, the modified Borg dyspnea scale (mean value of assessments at ~5, ~10 and ~15 days). Patients who are enrolled as inpatients and discharged within 24 hours of receiving the first dose of the study medication were ranked similarly to outpatients.

The ranked severity score has several advantages compared to binary outcomes (e.g., all-cause death) or time-to-event outcomes (e.g., time to death).²³⁻²⁵ It incorporates information about each of the highest-priority events in COVID-19, but allows these events to be prioritized within a single endpoint. For instance, the principal outcome of interest is death, but even if there is no difference in rate of death, we would still be interested in a shorter duration of invasive respiratory support, a shorter duration of hospital admission with better oxygenation parameters, and so on. This maximizes study power and minimizes the number of participants that need to be enrolled in order to detect clinically-meaningful differences.

Secondary and exploratory endpoints

Secondary endpoints were as follows: (1) the number of days alive, out of the intensive care unit, free of mechanical ventilation (invasive and non-invasive), extracorporeal membrane oxygenation (ECMO) or maximal available respiratory support in the 30 days following randomization; (2) a seven-category ordinal scale consisting of the following categories: not hospitalized with resumption of normal activities; not hospitalized, but unable to resume normal activities; hospitalized, not requiring supplemental oxygen; hospitalized, requiring supplemental oxygen; hospitalized, requiring nasal high-flow oxygen therapy, noninvasive mechanical ventilation, or both; hospitalized, requiring extracorporeal membrane oxygenation (ECMO), invasive mechanical ventilation, or both; and, death; (3) a ranked severity score similar to the primary endpoint, but using a more comprehensive COVID-19 symptom scale instead of the dyspnea Borg scale (Appendix 1).

Exploratory endpoints included: (1) time to all-cause death; (2) time to hospitalization (among participants enrolled as outpatients); (3) time to discharge (among participants enrolled as inpatients); (4) the number of days alive and out of the hospital during the 30 days following randomization; (5) a ranked severity score similar to the primary endpoint, but built only with factors 1-4.